Chapter 9

Three-Dimensional Reconstruction and Stereoscopic Display of Neurons in the Fly Visual System

ROLAND HENGSTENBERG, HEINRICH BÜLTHOFF
and BÄRBEL HENGSTENBERG

Max-Planck-Institut für biologische Kybernetik
Tübingen, F.R.G.

Introduction

Nerve cells are complicated anisomorphic bodies, intertwined amongst thousands of others. Their structural complexity is apparently crucial for their function and, therefore, the function of the nervous system as a whole. However, it is notoriously difficult to visualize the three-dimensional structure of nerve cells and their spatial relationships within different brain regions (His 1887).

We present a straightforward and simple procedure for three-dimensional display of structures from serial sections. We use the human brain for the most difficult part of the work; recognizing contours, aligning sections and perceiving depth by stereopsis. The boring and laborious part of the work (labelling, noting, handling and storage of large amounts of data) is left to a minicomputer with standard peripheral equipment. In its present form our procedure does not require sophisticated subprograms. These can, however, be implemented if required. General aspects of computer-aided neural reconstruction and solutions of special problems are described by Gaunt and Gaunt (1978), Lindsay (1977), Macagno et al. (1979), Sobel et al. (1980) and Ware and LoPresti (1975); see also Chap. 8, this Volume.

Procedure

Our procedure, initiated in 1975, is based upon manual reconstruction of stained neurons, consisting of the following steps: (1) intracellular penetration and recording; (2) fluorescent dye injection (Procion yellow M4-RAN; Stretton and Kravitz 1968, or Lucifer yellow CH; Stewart 1978); (3) histological processing (fixation, dehydration, infiltration with paraffin and serial sectioning at 7–10 μm); (4) fluorescence photography on Kodak EHB 135 at a magnification of 40×–60× with high aperture fluorescent microscope lenses (Zeiss, Universal microscope, incident light illuminator III RS,

N. J. Strausfeld (ed.), *Functional Neuroanatomy*

Neofluar 16/0.5 W-Oil, 25/0.8 W-Oil; (5) sequential projection and manual alignment of slides on a digitizer tablet (Fig. 1); (6) drawing and simultaneous digitizing of contours with a data acquisition program (HISDIG); and (7) transformation and reproduction of digitized structures with a transformation program (HISTRA). Steps 1–4 have previously been published in detail (Hengstenberg and Hengstenberg 1980).

Our procedure should be usable without special knowledge of computers; it exploits the operator's image processing capabilities for contour extraction, section alignment and depth perception by stereopsis. Data acquisition is ergonomic in that structures can be digitized as they would be drawn, including their fine details. During drawing, the operator is not loaded with additional computer chores. Resolution is preserved and alignment between sections utilizes the present state of the reconstruction rather than only the preceding section. Data and program structures allow later implementation of other more sophisticated evaluation routines. We do not use expensive hardware such as image processors for real-time image transformation and display, nor do we use highly sophisticated software for reconnecting cut fibres, hidden-line removal, shading or plane-surfaced polyhedra (see Chap. 8 this Vol.). Instead we explore how much of an "ideal" three-dimensional reconstruction of neurons can be achieved by high resolution stereograms of the raw data, and image processing by the human brain in stereopsis.

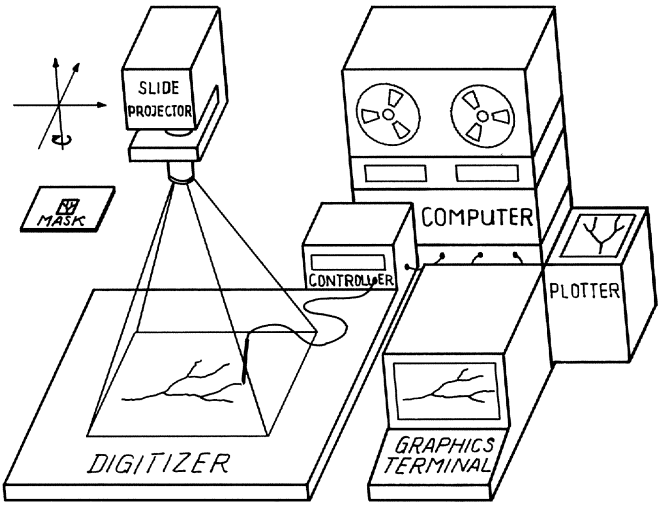

Fig. 1. Hardware configuration. Colour slides of sections are projected at about 600× total magnification by an adjustable slide projector onto a large digitizer tablet, covered with drawing paper. Contours are drawn, and simultaneously digitized, fed to a minicomputer and displayed on a graphics terminal which also serves to control acquisition and reproduction programs. Final graphs are produced by an electrostatic printer/plotter

Hardware Configuration

Hardware (Fig. 1) consists of a slide projector (24 × 26 mm), mounted on an adjustable gimbal. Slides are aligned by an adjustable mask and projected onto a large digitizer tablet (Summagraphics ID-RS232; 70 × 120 cm) whose surface is covered with drawing paper. Contours are drawn with a colour pen while being digitized (30 x,y-values per s). Contour data are fed (via a microprocessor-controlled buffer memory, 32 Kbyte) to a general purpose minicomputer (Digital Equipment, PDP 11/34), and are preprocessed and stored on magnetic disc (CDC 9762; 80 Mbyte) or tape (Kennedy 9000; 9 tracks, 800 bpi). Digitized contours are plotted on-line on a storage tube graphic display (Tektronix 4006) next to the digitizer, so that the operator can see and perform necessary corrections in real time. The terminal also serves to control the data acquisition program HISDIG. Stored data are processed by an evaluation program HISTRA and plotted on an electrostatic printer/plotter (Gould 5200; 20 × 30 cm; 80 dots cm^{-1}).

The Data Acquisition Program HISDIG

Data acquisition is in principle similar to manual drawing. Its major features are outlined below.

Data Specification

The first part of HISDIG specifies the data file (filename, storage location, field size, thickness of sections etc.). It further accepts a list of 20 identification codes (ID) for structures to be handled separately (e.g. neuropil surface, fibre tracts, stained and unstained neurons etc.). A resolution increment (RI), specified for each identification code, determines fine (stained cells) or coarse (brain outline) digitization. This has the advantage of saving memory space and reconstruction time for contours with low information content. HISDIG is now ready to accept data and asks for the first section and ID-code.

Digitization of Contours

While the projected image is being traced, the digitizer continuously samples the pen location and yields data points (x, y) with a resolution of 0.1 mm at a rate of 30 points s^{-1}. Together, with the section number and thickness, these coordinates define a point in space P (x, y, z). Subsequent data points are stored by the computer only if they are more than one resolution-increment (RI) away. By appropriate choice of RI for each of the

structures to be digitized, an adequate resolution can be maintained for coarse and fine structures without accumulation of redundant data.

Data points separated by more than two RIs are interpreted as the end of one and the beginning of a new contour, i.e. a new profile of the same structure. To reconstruct contours, subsequent data points are joined by a line, as long as their distance $D < 2RI$. When $D > 2RI$, no connecting line is drawn, and profiles remain separate. The advantage of this is that many complicated profiles may be digitized without having to converse with the computer. This means that outlines can be drawn in any sequence, even arbitrary segments of one profile. This is practical since few people can draw lines accurately in every direction. Unlike automatic contour tracing systems (see Sobel et al. 1980) our semi-automatic system needs neither expensive hardware nor sophisticated software.

Alignment of Sequential Sections

The most crucial step in serial section reconstruction is alignment of sequential sections. For this we use the most fancy, fast and foolproof image processor (FFFIP) which is presently available: the operator's brain (see also Chap. 8, this Vol.).

We do not usually start reconstruction with the first or last section of the series, but begin with a middle section containing many stained profiles and having the largest brain area. This achieves optimal placement of the reconstruction, with respect to field boundaries. The wealth of detail in this initial section facilitates alignment of subsequent sections, especially if the stained profiles (or other prominent landmarks) are scattered. It is then very easy for an experienced operator to align the first few sections perfectly, even though the reconstruction is still quite fragmentary. At this stage, it is also useful to draw auxiliary structures that are not to be digitized to aid alignment. Later, the alignment of a section is quite easy because it matches not only the adjacent section, but all previously drawn structures. This minimizes the risk of cumulative errors such as linear shift or "helical distortion". As luck has it, sections of important preparations tend to be technically imperfect, i.e. they may contain folds, scratches, tears or bits of dirt. At worst, a section may even be missing. Even using the whole reconstruction as the reference frame for alignment one cannot eliminate such flaws, but it obviously helps the operator to make appropriate corrections.

The upper- and lowermost sections of a series usually contain only fragments of a stained cell and often very little of its environment. With an almost completely drawn reconstruction, it is usually no problem to fit in small fragments.

Correction and Storage of Data

Data are automatically saved on magnetic disc, and data acquisition can be interrupted whenever all contours of one ID-code are digitized. Should the computer break down, all data, except for those of the ID-code presently being digitized, are saved. Such an emergency, or if the computer is needed for other purposes, does not require that the work is repeated.

If during a reconstruction, certain data are incorrect (e.g. inappropriate matching of profiles), that section and ID-code can be called and digitized again. The incorrect data are automatically erased.

Data generated by HISDIG are stored on magnetic disc for fast access until the desired reconstructions and graphs are completed. Then they are compressed and stored on magnetic tape. They can be updated and compared with other preparations. On average a preparation requires < 1000 blocks of 256 words. Our largest data file is < 3000 blocks.

Field Size and Resolution

The present set-up was developed for our particular research on the fly's brain (Hengstenberg et al. 1982). It is, however, generally applicable. Other magnifications of microscope or projection yield various trade-offs between field size and resolution. The figures in Table 1 emphasize that the resolution of the fluorescence microscope is preserved throughout the reconstruction procedure and is still present in the stored data (Table 1, rows a–d). This is done by using a large digitizing tablet, which, at an overall magnification of about 600 ×, allows one to draw and digitize profiles of < 1 μm diameter. When reconstructions are plotted or printed, considerable loss of resolution occurs due to the limited resolution of these processes (Table 1, row e). This is pronounced when the whole field of 1200×1800 μm

Table 1. Field size and resolution

		Width	Length	Resolution	Frames per section	Data per section
a	Largest section size	1200 μm	1800 μm	–	1	–
b	Field (Neofluar X 16/0.5)	600 μm	900 μm	0.55 μm	4	7.1×10^6
	Colour film	24 mm	36 mm	15 μm	4	15.4×10^6
c	Field (Neofluar 25/0.8)	400 μm	600 μm	0.35 μm	9	17.6×10^6
	Colour film	24 mm	36 mm	15 μm	9	34.7×10^6
d	Digitizer tablet	700 mm	1050 mm	0.10 mm	1	73.5×10^6
e	Gould plotter	190 mm	280 mm	0.15 mm	1	2.4×10^6
	Printed stereograms	50 mm	75 mm	0.10 mm	1	0.4×10^6

is displayed. However, smaller fields of $500 \times 700\ \mu m$ can be plotted or fields of $200 \times 300\ \mu m$ can be printed without loss of resolution. It is therefore necessary either to compromise between field size and resolution (Figs. 3, and 5–11) or to divide plots into survey and detail pictures (Fig. 4).

The Reproduction Program HISTRA

Digitized data are reproduced by a second program specifying: (a) digitized structures to be reproduced or omitted, as selected by their ID-code; (b) part of the preparation (length, width, depth) to be evaluated (three- dimensional window); (c) shift along x-, y-, z-axes; (d) rotation in space about x-, y-, z-axes; (e) linear scaling along individual axes; (f) perspective, i.e. choice of viewing distance; (g) choice of two-dimensional reproduction (shadowcast from a specified viewpoint) or three-dimensional reproduction by computation of stereo pairs; (h) type of contour line for different structures (e.g. light/heavy or dotted, broken, solid or colour), and the plotting device (graphic terminal or plotter).

HISTRA further accommodates a variety of subprograms for quantitative evaluations (contour length, profile area, cell volume etc.). A particularly important aspect of data transformation is computation of stereo pairs for viewing digitized structures in three dimensions.

Stereoscopic Vision

Euclid (280 BC) stated that "stereopsis" (Greek: solid sight) is caused by the simultaneous impression of two dissimilar images of the same object in the two eyes (Okoshi 1976). This dissimilarity is illustrated in Fig. 2a for three points of an object. When the eyes are fixed on the cross, it will be focussed by the lenses onto corresponding locations in the foveae of the two eyes. Other points in the fixation plane (horopter) will be focussed onto corresponding but laterally displaced locations. However, points behind or in front of the fixation plane are projected onto noncorresponding ("disparate") locations (Fig. 2a). This disparity (amongst several other cues) is used by the stereoprocessor in our brain to compute the depth of an object relative to the plane of fixation, where the disparity is zero. This trigonometric calculation is simple if there are only a few objects in the surround, but it becomes most difficult for many objects as in a natural scene, or in some of the stereograms presented in this article. In those cases, the brain must first solve the "correspondence problem," i.e. it has to work out which image points in the two eyes belong to which object point. This problem is clearly illustrated by Frisby (1979); Marr and Poggio (1976, 1979) suggest how the brain may solve it.

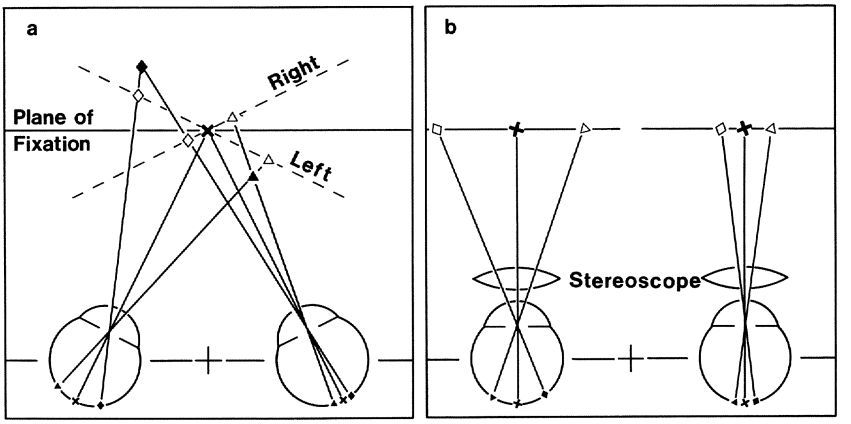

Fig. 2a, b. Stereoscopic vision. **a** Projection of points in space (◆, ×, ●) onto the two retinae, while fixating an object. Notice that the fixated point (×) is focussed onto corresponding locations of the two retinae, whereas points in front or behind the plane of fixation are projected onto noncorresponding ("disparate") locations. The disparity between left and right retinal image is used by the brain to perceive depth. The oblique lines (*Left, Right*) denote those planes into which the object points are projected to generate the two half-images of a stereogram (◇, ×, △). **b** When a stereogram is viewed with a stereoscope, the projected points in the half-image are focussed onto the same (disparate) locations of the two retinae as when looking at object points in different depths. Consequently such image points are perceived to have the same depth as the real object points

The construction of stereograms mimics the optical transformation of points in space, as they would be seen by two laterally separated eyes. This may be achieved by tilting the object or the assembly of data points P (x, y, z) by $+2.5°$, and projecting all points into a plane normal to the line of sight. This yields the "half-image" for one eye and repeating the procedure with $-2.5°$, the half-image for the other eye. A disparity angle of $\pm 2.5°$ is equivalent to a fixation distance of 75 cm. A nonlinear disparity correction (Glenn and Burke 1981) is in our opinion not necessary.

The two half-images have to be presented independently to the two eyes by a stereoscope. The brain will then solve the correspondence problem and thereafter compute the appropriate depth for all pairs of image points (Fig. 2b). When the sign of the disparity angle is reversed either by computation or by exchanging the two half-images, the depth sensation reverses also, and objects may be viewed "from the other side" (Figs. 6, 7).

Stereoscopes

Stereoscopic vision requires that the two half-images are independently presented to the two eyes. This can be achieved in different ways:

a) *Anaglyphs:* red and green half-images are printed in register and viewed through red/green spectacles so that each eye sees only one of the stereo

pair. Anaglyphs can be viewed directly and printed if colour facilities are available (see Fig. 10. Chap. 7. this Vol.).

b) *Mirror stereoscopes* of 220 mm base are best suited for direct inspection and stereometry of large-format stereograms (20 × 30 cm each half-image) such as are obtained directly from the plotter. Mirror stereoscopes are available from C. Zeiss, Oberkochen, Germany, mod N2; Balzers AG, Lichtenstein, mod SB180.

c) *Lens stereoscopes* are useful for small stereograms of 65 mm basis as in Figs. 4–12. They are available from C. Zeiss, mod TS4, order no. 516404; or from Edmund Scientific Corp. Barrington, N.J., USA, order no. 42118. Note: The addition of convex lenses considerably improves the depth perception because the virtual images of the stereo pair are now located several meters ahead and therefore accommodation of the eyes becomes less effective as a cue for depth perception.

d) *Improvisation of a lens stereoscope:* mount two lenses of 90–150 mm focal length (ca. 30 mm diameter) 55–65 mm apart, so that their optical axes are parallel. Mount them about 1.1 focal length above the stereogram, so that both planes and the baselines are parallel. Stereopsis may also be achieved without a stereoscope by uncoupling of convergence and accommodation of the eyes.

e) *Slide projection* of anaglyphs is possible by two aligned projectors and red/green filters; colour matching may, however, be critical. Stereograms may be similarly projected through crossed polarizers onto a metallic screen and viewed through polarizer spectacles.

Stereopsis for Beginners

The stereoscope must be parallel with respect to the baseline of the stereogram. It may be shifted up/down or left/right to scrutinize details. Tilting, however, creates vertical disparities which are "unfamiliar to our brain" and which spoil stereopsis straightaway. Stereopsis is usually not achieved immediately (Julesz 1971) and may take up to 10 min to achieve. The intensity of depth perception increases gradually during this time, and many details become visible only towards the end of this period. This slow and gradual increase of depth perception is particularly conspicuous when looking at the stereogram for the first time. Fixate patiently a central area and view relaxedly. Observers with glasses should wear them.

Examples of Displays and Stereopairs

The directional preference of certain wide-field movement-sensitive interneurons in the fly visual system is correlated with their location within the neuropil: horizontal cells (HS) are in the anterior surface layer, and vertical

cells (VS) are in the posterior surface layer of the lobula plate (Hausen 1981). It was, however, not clear whether or not this correlation holds also for other types of cells. Furthermore it was not clear how neurons with apparently "oblique" preferred directions (Hausen 1976a, b; Eckert and Bishop 1978; Hengstenberg 1981) are arranged in the neuropil. We therefore combined intracellular studies on the directional specificity of neurons with three-dimensional reconstruction to clarify the spatial organization of the lobula plate. For this it was not only necessary to reconstruct the stained cells "floating in vacuo," but also to show their spatial relationship to adjacent identifiable neurons and to the neuropil boundaries. At the same time, already available knowledge about many of these neurons could be utilized to develop and evaluate this procedure.

The examples of stereopairs (Figs. 4–12) ought to be viewed with a lens stereoscope. For readers with an impairment of stereopsis the text describes what can be seen. It should be kept in mind that bookprinting can seriously reduce resolution (cf. Table 1).

Selective Display

Selective staining procedures often show a preference for particular neurons or cell classes. Neurons which are refractory to such procedures will therefore remain concealed. Reconstructions from unspecifically stained semithin serial sections may be used to reveal the presence, shape and location of such cells. Figure 3 shows two plots, where 27 comparatively large tangential neurons in the lobula plate of the blowfly were reconstructed from 85 sections of 3 μm thickness. Contrary to all other reconstructions shown later, the cells were not reconstructed on a single sheet of drawing paper but on a stack of prealigned foils. Plotting all neurons simultaneously (Fig. 3a) yields a chaos which cannot be disentangled. By plotting only a few neurons, (as selected by their identification codes) at a time, and by employing various combinations, it is possible to reveal the structure of single neurons, their location in the neuropil, and their relative position with respect to other identifiable cells (Fig. 3b). By this procedure, it was also possible to confirm the existence of a particular neuron (VS1) in the blowfly (Hengstenberg et al. 1982), which had previously been described in the housefly (Pierantoni 1976), but had never showed up in cobalt mass-impregnations of VS-cells (Hausen et al. 1980).

Survey and Detail

Nerve fibres are usually long and thin and may have fine arborizations in different, widely separated neuropils. It is impossible to display such neurons in toto and with sufficient detail. Our scheme of digitizing with high

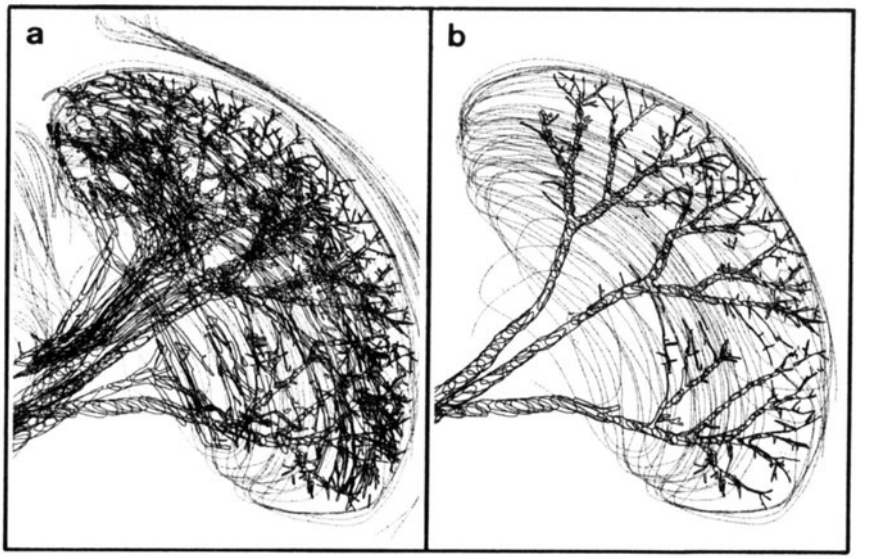

Fig. 3a, b. Selective display. Twenty-seven tangential neurons in the lobula plate were reconstructed from 85 unspecifically stained semithin sections in order to map the number, position and structure of neurons accessible for microelectrode penetration. **a** Displaying all reconstructed cells is a useless chaos. Displaying only a few at a time, as selected by their name (Identification Code), and in various combinations, allows recognition of identifiable neurons, clarification of their relative positions, and statements about the existence, shape and position of neurons which have so far not been impaled. **b** shows as an example the three horizontal cells HSN, HSE and HSS as selectively displayed from the data file of **a**. Field width 480 μm. Neurons in Figs. 3–11 are from *Calliphora erythrocephala*

resolution on a large tablet allows low resolution survey plots with data compression and recovery, when necessary, of high resolution by magnification of particular regions. This is not to be confused with photographic enlargement, where just the scale is blown up. Figure 4 shows a heterolateral projection neuron (H4) of the fly visual system with three distinct arborizations: one in the lobula plate, another in the ipsilateral protocerebrum, and a third in the contralateral posterior slope. Figure 4a shows the whole neuron in a generalized neuropil outline, which was digitized along the largest circumference of different neuropils (cf. Fig. 3). Figure 4b is a stereogram of the contralateral axonal arborization, magnified $\times 2.2$. The axon is about 5 μm in diameter where it enters the plot, and the small collaterals are about 1 μm or less in diameter. The contour jitter of about 0.2 μm demonstrates the resolution limit of digitization, in part due to the drawer's tremor, and in part due to the resolution limit of the digitizer tablet (0.2 μm). The stereogram reveals that the telodendritic arborization extends through a volume of about $200 \times 220 \times 150$ μm and where each single collateral is located in this volume. If another neuron passing through this region had been stained, a

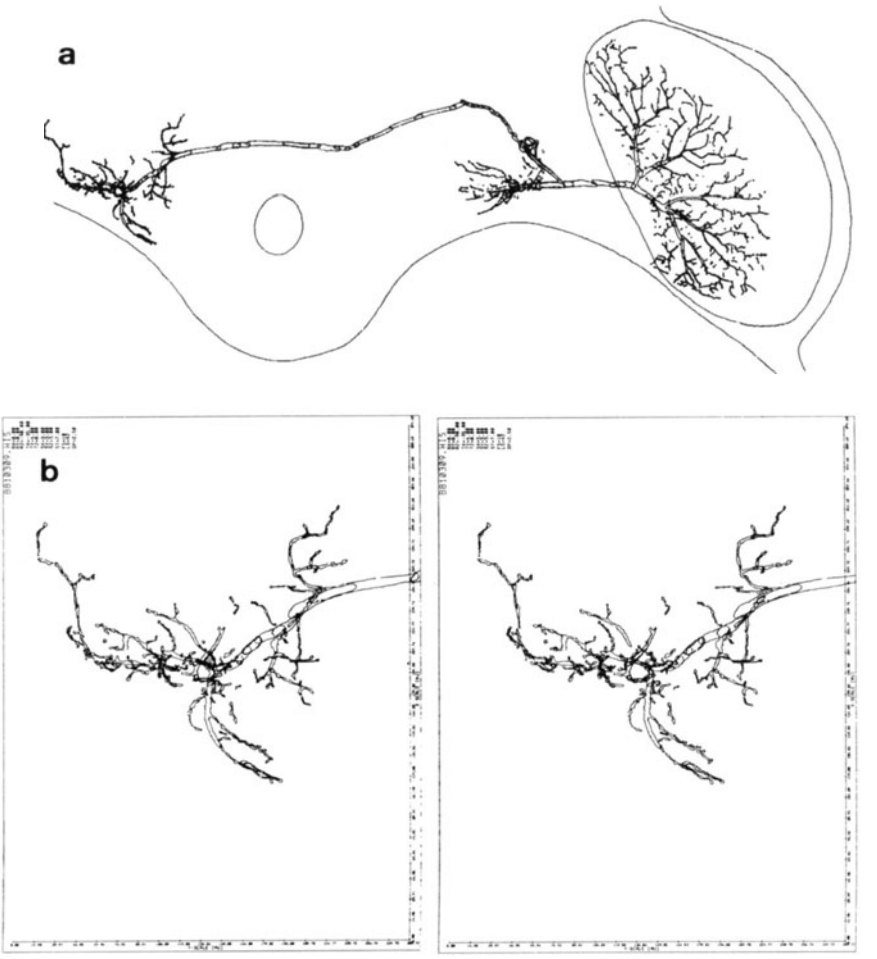

Fig. 4a, b. Survey and detail. **a** Survey picture of the heterolateral projection neuron H4, as seen from behind. The cell has three discrete arborizations, one in the right lobula plate, another in the ipsilateral protocerebrum, and a third in the contralateral posterior slope. **b** Stereogram of the contralateral, presumably telodendritic arborization of H4, seen from behind. Field width: **a** 1250 μm; **b** 285 μm. This high-resolution stereogram was generated by the window function of the reproduction program HISTRA, retrieving the full information about a small area from the data file of the whole cell. The axon is about 5 μm, most collaterals are about 1 μm in diameter

fair estimate could have been made about the proximity of the two neurons, and if collaterals were possibly involved in contacts. It should be kept in mind that selection of the area to be plotted is a function of the reproduction program HISTRA, operating upon stored data. There is no need to do the tedious reconstruction again.

Depth Interpolation by Stereopsis

We compute and display stereograms from incoherent contour data. This means that contours in one section are compressed into a plane and subsequent sections are represented by a series of such "contour-planes," each separated by an empty space of section thickness. One would therefore expect to see in the stereograms piles of irregular squiggles, separated from one another. This is in fact true for coarse structures like neuropil outlines. Reconstructed neurons, however, are remarkably coherent and smooth. Apparently our stereoprocessor interpolates between different contour planes if there is no doubt about the local correspondence. This fortunate property allows us to do without any advanced subroutines to reconnect cut profiles or to suppress "hidden contours". Figure 5 shows the dendritic arborization of the tangential neuron H2 and the outlines of the right lobula plate, as seen from the front. H2 responds selectively to horizontal back-to-front movement in the ipsilateral visual field. The arborization is essentially flat and closely apposed to the anterior surface of the neuropil. This is best seen in the upper part of Figure 5, where sufficient contour lines of the lobula plate are present.

Functional Stratification

Previous studies on the fly visual nervous system (Eckert 1979; Hausen 1976a, b, 1981; Hengstenberg et al. 1982; Pierantoni 1976; Strausfeld 1976) have shown that the location of tangential cells in the lobula plate is correlated with their characteristic response properties. Cells which respond best to horizontal movements in the visual field are located in the anterior surface layer of the lobula plate, and cells which respond best to vertical movements are located in the posterior surface layer. Figure 6 illustrates this correlation for two types of large movement-sensitive tangential cells. The upper part of Fig. 6 shows a stained horizontal cell (HSN) digitized together with the unstained profiles (fluorescence shadows) of horizontal (HS) and vertical cells (VS). It shows further the outlines of the right lobula plate neuropil, as seen from behind. The stained HSN and unstained HS profiles appear to lie deeper, i.e. they are closer to the anterior surface. The unstained VS-profiles "float" on top, close to the posterior surface of the lobula plate. The lower part of Fig. 6 illustrates the reverse situation: a giant vertical cell VS4, in the left lobula plate is viewed anteriorly. Like the VS-shadows in Fig. 6a, its main branches are closely apposed to the posterior surface of the lobula plate, and the small dendritic branches extend mostly towards the observer, i.e. into the neuropil. Such reconstructions of single stained neurons together with profiles of unstained but identifiable cells and the neuropil boundaries allow us to generalize the correlation between location in the neuropil and functional specificity. The horizontal movement-sensitive neuron H2 (Fig. 5) and several other tangential cells (not shown) obey this rule.

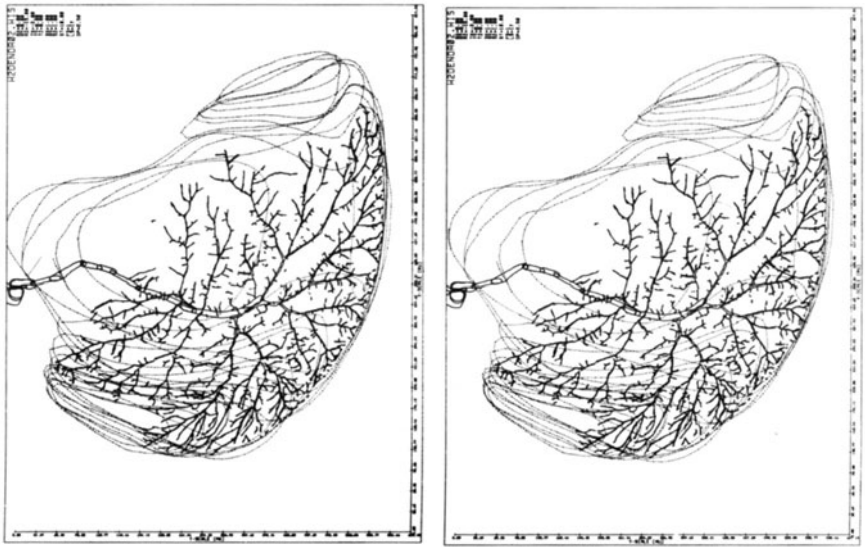

Fig. 5. Depth interpolation by stereopsis. Dendritic arborization of interneuron H2 in the right lobula plate, as seen from anterior. The bulge of the lobula plate towards the right indicates the large fibre tracts leaving the neuropil. Field width: 620 μm. Notice the coherent and smooth appearance of the arborization, even though no subprograms for reconnection of cut profiles or hidden line removal have been applied

Synaptic Contact Layers

The correspondence between the physiological specificity of neurons and their location within the neuropil, as stated so far, may be misleading if only the location of the main branches is considered. This is due to the fact that the vast majority of synaptic contacts is found on the outermost dendritic branchlets (Pierantoni 1976; Hausen et al. 1980; Bishop and Bishop 1981). In HS- and VS-cells these branchlets extend more or less distinctly towards one another (Fig. 6) and may in principle form either distinct "horizontal" and "vertical" synaptic contact layers, or they may approach and penetrate one another to form a mixed layer. By sequential penetration, dye injection and three-dimensional reconstruction, this question can be unambiguously answered. Figure 7 shows two stereograms of the horizontal cell HSE (Figs. 3, 6) and of the vertical cell VS2; in the upper one, as seen from posterior, and in the lower, as seen from anterior. As in previous figures, the main branches are seen to lie in the anterior and posterior surface layers of the lobula plate, and the small dendrites extend towards the interior of the neuropil. In the region of overlap the small dendrites of both cells form discrete layers separated by an empty space. Not a single dendritic branchlet of either neuron invades "foreign territory." This finding is consistent with results

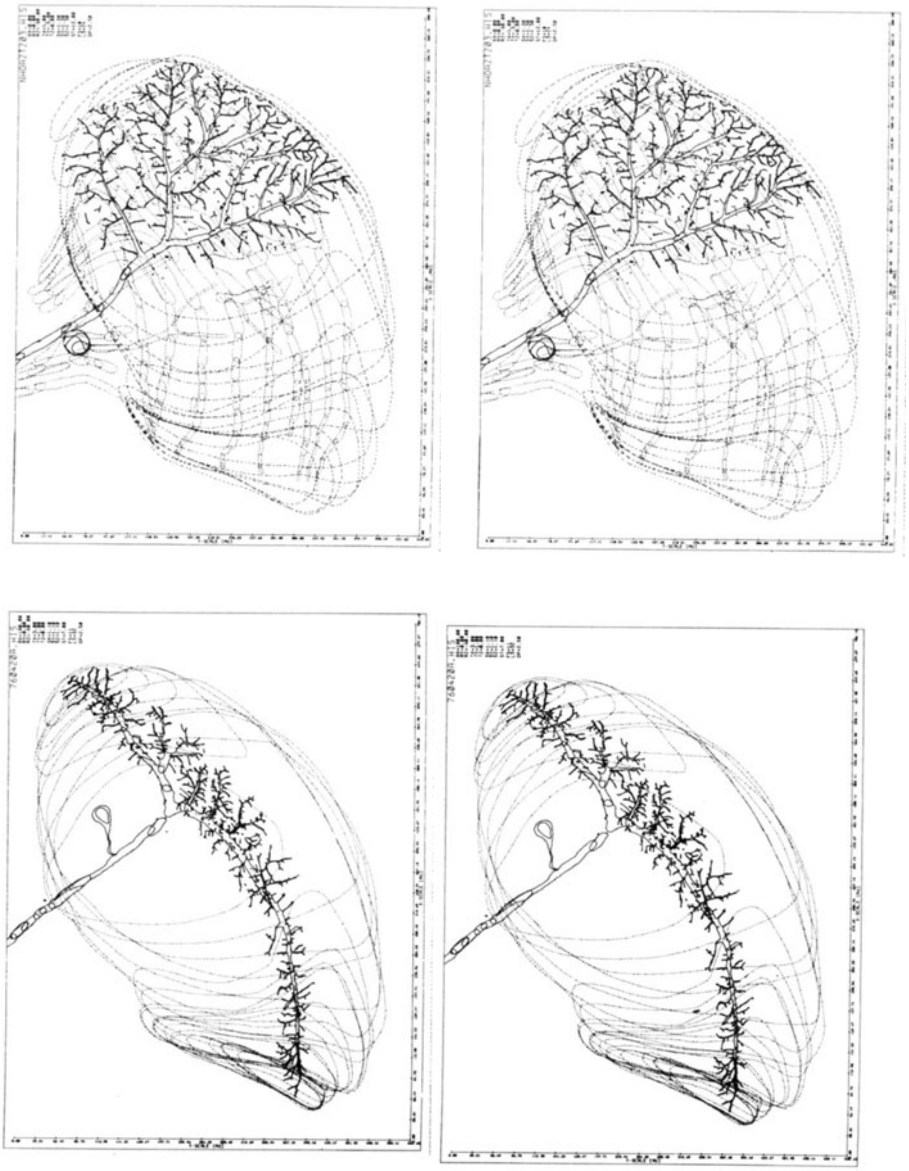

Fig. 6. Functional stratification. *Top* Dendritic arborization of neuron HSN, together with unstained profiles of HS-, and VS-cells, and the outlines of the right lobula plate; seen from posterior. *Bottom* Dendritic arborization of neuron VS4 in the left lobula plate, seen from anterior. Field width: *top* 450 μm; *bottom* 550 μm. The lobula plate appears like a thick-walled transparent bowl; stained neurons float inside the "wall;" vertical cells are apposed to the posterior (outer) surface of the neuropil and horizontal cells are apposed to the anterior (inner) surface. Compare Fig. 5: H2, which also responds specifically to horizontal movements

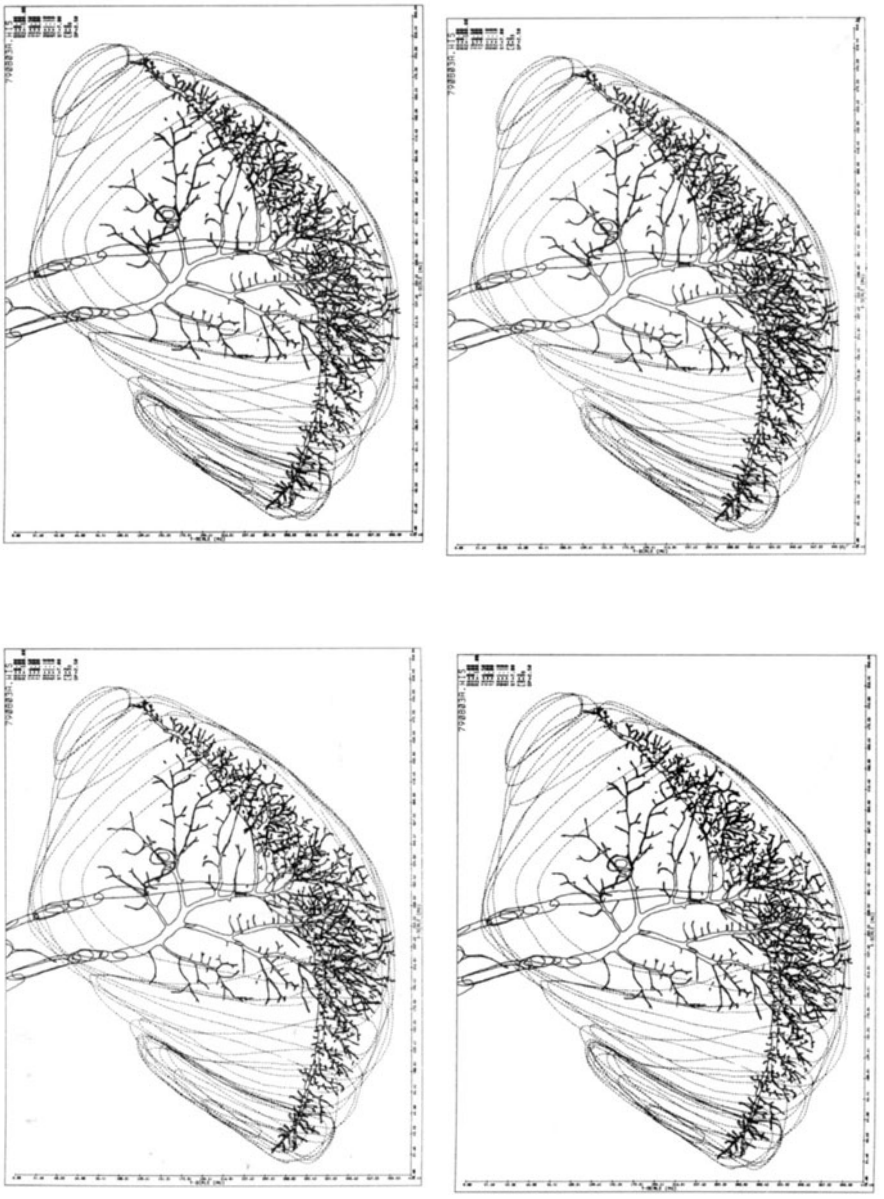

Fig. 7. Synaptic contact layers. A horizontal cell HSE and a vertical cell VS2 stained and reconstructed from the same fly. *Upper stereogram*, is seen from posterior; *lower* is seen from anterior. Field width 420 μm. Notice the location of main branches, and the perfect separation of small dendritic branchlets of the two neurons. This corresponds to directional specificities to wide-field movements in the visual field. Compare also the different attractiveness of structural features in the two stereograms

from cobalt mass-impregnations (Strausfeld and Obermayer 1976; Hausen et al. 1980). The conclusion that there are discrete synaptic contact layers, specified by their directional specificity was recently corroborated by ^{3}H-2-deoxyglucose labelling under specific stimulation and subsequent high-resolution autoradiography (see Chap. 11). Figure 7 also illustrates how much more information can be retrieved from a stereogram than from the same graph viewed two-dimensionally. It shows further that even in this case of dramatic overlap, hidden-line removal is not necessary to perceive the structural relationships between the two neurons.

The two stereograms of Fig. 7 are identical except for the sign of disparity. Therefore they are excessively redundant and one would not expect them to provide different insights. It is, however, interesting to compare the two stereograms and to observe how attention is attracted to different structural features when looking from anterior or posterior into the same structures. Apparently, attention is mainly guided to objects in the foreground.

Bistratified Vertical Cells

Some of the tangential neurons in the lobula plate do not exhibit a clear-cut preference for either horizontal or vertical movements in the visual field

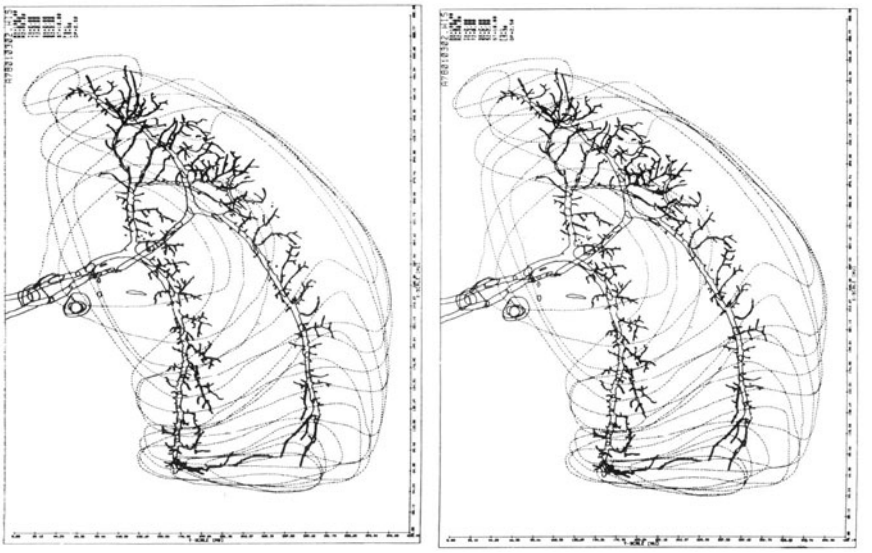

Fig. 8. Bistratified vertical cells. Two vertical cells, VS4 and VS8 from the same fly, as seen from anterior. Stereo effect overemphasized by computation with 1.5 × real section thickness. Field width: 420 μm. VS4 (*right*) is entirely confined to the posterior layer of the lobula plate, and responds exclusively to vertical movement. VS8 (*left*) is bistratified: its ventral dendrites are in the same layer as VS4, but the dorsal dendrites invade the anterior layer of horizontal cells (cf. Figs. 5–7). Local movement stimuli in respective parts of the visual field reveal that local directional specificity correlates with dendritic stratification

(Eckert 1979; Hausen 1976b, 1981; Hengstenberg 1981). The vertical cells respond in different ways to horizontal and vertical movement. Three-dimensional reconstruction of such neurons shows that the dendritic arborization of VS1 and VS6–VS10 is bistratified. Figure 8 shows an example of this arrangement. As in Fig. 7, two neurons, VS4 and VS8, were successively impaled in the same animal, studied physiologically and injected with Procion yellow. VS4 is exclusively excited by downward movement, whereas VS8 responds to downward movement and to front-to-back movements. The former response dominates in the ventral half of the visual field and the latter in the dorsal half. The stereogram (Fig. 8) shows clearly that VS4 is monostratified and resides entirely in the posterior surface layer of the lobula plate. VS8, however, is not confined to one neuropil layer: in the ventral part of the lobula plate it resides in the posterior layer but in the dorsal half it occupies the frontal surface layer, as if it were a horizontal cell. Here again the small dendritic branches apparently invade discrete layers of the neuropil presumably because appropriate input information is available only there.

From the retinotopic mapping of the visual field into the lobula plate, combined with the local directional preference of a neuron, flight manoeuvers of the fly can be inferred that would maximally excite such neurons. VS8 is expected to respond best during pitch movements about the transverse axis of the fly.

Intermediately Located Neurons

The examples of neurons presented so far (Figs. 5–8) seem to suggest that entire tangential cells or parts of them are located either in the anterior or in the posterior layer of the lobula plate. There are, however, other neurons which occupy intermediate positions (Hausen 1981). Figure 9 shows as an example the arborization of H4 in the lobula plate (Fig. 4). It is displayed together with the fluorescence shadows of HS-, and VS-cells. With some scrutiny, its intermediate position between the two cell classes can be recognized. Interestingly, its small branchlets extend both ways, anteriorly as well as posteriorly, and the cell responds well to oblique movements from postero-superior to antero-inferior in the ipsilateral visual field. Even though the spatial arrangement of H4 differs in principle from the previous examples, the correlation between its structure and function suggests that directionally specified input elements are organized in discrete layers.

Sequence of Neurons

A central problem of neuroanatomy is that of synaptic connectivity. Which neurons converge upon which subsequent ones? Figure 10 shows again two

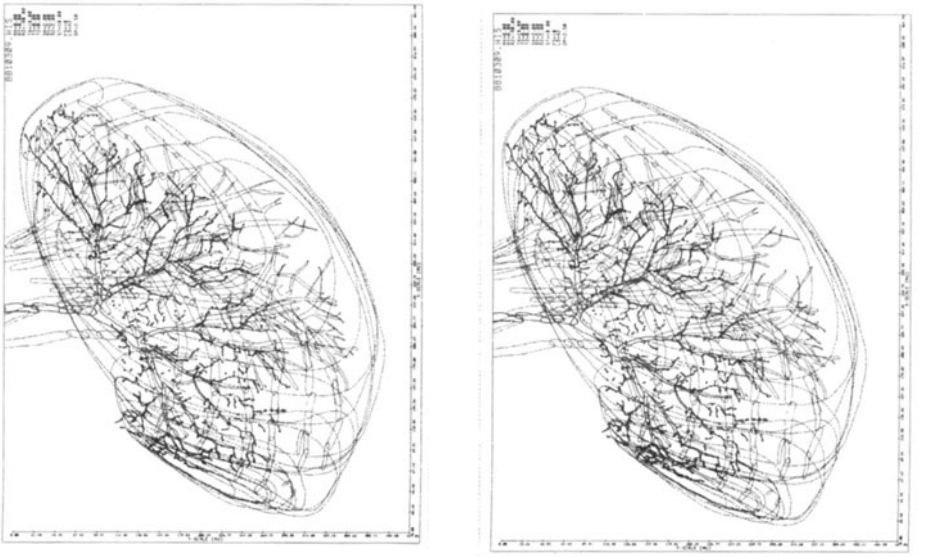

Fig. 9. Intermediately located neuron. Arborization of H4 (cf. Fig. 4) in the right lobula plate seen from posterior. Field width 430 μm. The axon and major branches lie between the fluorescence shadows of HS- and VS-cells. Small branches extend both ways: anteriorly into the layer of horizontal cells, and posteriorly into the layer of vertical cells. It responds best to oblique pattern movement

sequentially stained neurons of the visual system of the fly: a vertical cell VS9 (top), and a descending neuron YDN (bottom). Already the two-dimensional representation and even more so the respective stereogram (Fig. 10) show that the telodendritic arborization of VS9 and one of the two major dendritic branches of YDN are intimately intertwined. The second dendritic branch of YDN approaches large fibres of the ocellar system. Thus stereograms suggest sites of synaptic contact between branches of different neurons. They also draw attention to branches that seem to end blindly indicating additional inputs or outputs of neurons.

Neurons of Irregular Shape

The previous examples (Figs. 3–9) were all tangential neurons in the lobula plate of the blowfly. This neuropil has a highly ordered arrangement of retinotopic input elements (Strausfeld 1976). It is furthermore fairly shallow and essentially flat. It is therefore possible to select a plane of sectioning (frontal), where shadowcast reconstructions of the stained neurons represent reasonably well the structure of the neurons. The same would be true for Purkinje cells in the vertebrate cerebellum. In such cases the effort and cost of three-dimensional reconstruction may favour manual shadowcast reconstructions.

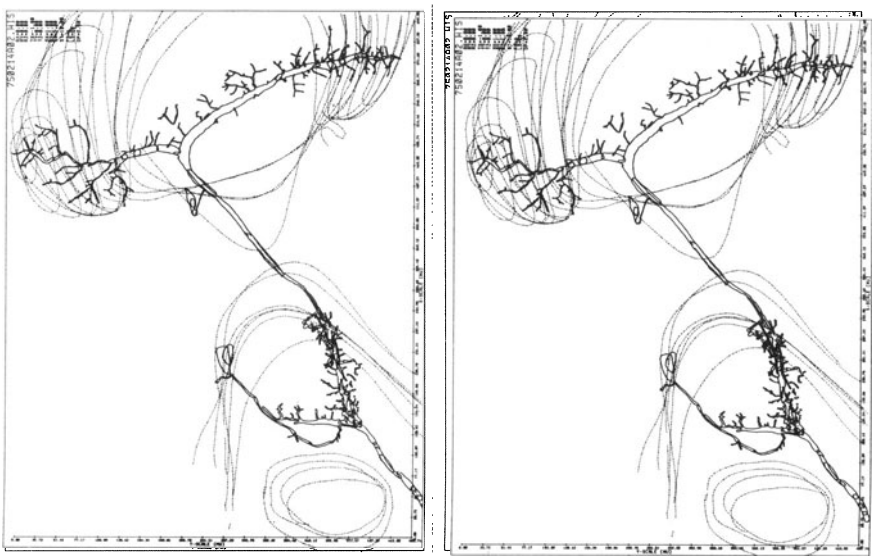

Fig. 10. Sequence of neurons. A vertical cell (VS9), and a descending neuron (YDN) were sequentially impaled and stained. The stereogram is rotated by 90 degrees (dorsal to the left) to utilize the print format optimally, and is seen from posterior. Field width: 500 μm. The terminal arborization of VS9 is in close contact with one dendritic branch of YDN, whereas the other approaches large fibres of the ocellar system (not shown). The axon of YDN, projecting into the mesothoracic neuropil is omitted. The close apposition of the two neurons suggests synaptic convergence but is of course not sufficient to prove contiguity. Stereograms of this kind show however those axon collaterals and dendritic branches which do not contact one another, thereby indicating additional inputs and outputs

The majority of neurons are however irregular in shape (e.g. stellate, granule and pyramidal cells of the vertebrate cerebral cortex, or interneurons and motor neurons of invertebrate ganglia). For these neurons it is impossible to define a unique plane of sectioning (e.g. a unique direction of view) representing the neuron in full detail. Single two-dimensional reconstructions of such neurons are necessarily ambiguous with respect to the orientation of their arborizations, and their three-dimensional structure can only be partly deduced by tedious orthogonal projections (Murphey 1973).

A large proportion of central interneurons connect particular neuropil areas, leaving others out. Single branches of such neurons may pass through well-known fibre tracts or less obvious routes. It is quite obvious that three-dimensional reconstruction and stereoscopic inspection of such neurons are well-suited for studying such complex arrangements. Figure 11 gives an example of such a neuron with irregular shape, extending into several different neuropil areas of the fly's protocerebrum. It is a descending neuron (DN3) whose axon leaves the brain about normal to the plane of view, close to the oesophageal canal, and then projects through the cervical connective to end bilaterally in the pro- and mesothoracic neuropils (Hengstenberg and

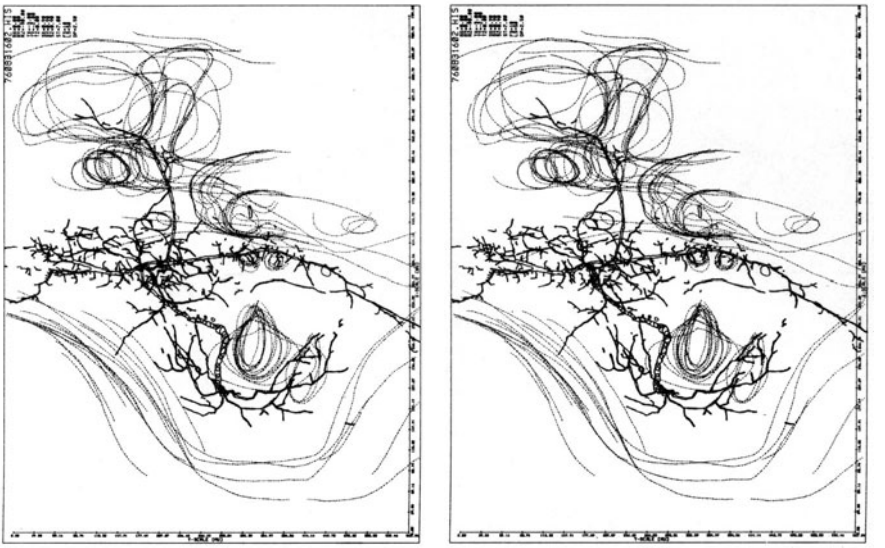

Fig. 11. Neurons of irregular shape. Dendritic arborization of a descending neuron DN3, seen from posterior. Field width 560 μm. Six major dendritic branches and the axon originate from a common branch point in the left lateral protocerebrum. Two project to the left and right optic foci through the posterior optic tract, one ascends towards the optic tubercle, bypassing the central complex and corpus pedunculatum, three smaller ones remain close to their origin in the lateral protocerebrum. In the uppermost section, the axon gives off a few collaterals which project bilaterally into the subesophageal ganglion. The axon projects then through the cervical connective bilaterally into the pro- and mesothoracic neuromeres (omitted). Obviously such complicated arborizations are best represented by stereograms

Hengstenberg 1980; Strausfeld 1976 plate 7.26 B). Figure 11 shows the dendritic arborization of DN3, and some of the protocerebral neuropil areas, as seen posteriorly. Near the cut end of the axon two collaterals arise and spread ipsi- and contralaterally into the optic foci of the posterior slope. Further up, the axon narrows down and divides into at least six major dendritic branches. Two prominent ones project either way through the posterior optic tract to lateral (presumably visual) parts of the protocerebrum. A third branch ascends ipsilaterally and projects to the optic tubercle, bypassing the central complex and the corpus pedunculatum, except for a small branch at the surface of the calyx. The remaining three main branches are confined to the ipsilateral protocerebrum; their precise destination is unknown.

Possibly, the complex structure of DN3 may correlate with quite complex (largely unknown) response properties: the cell is silent in the resting state and fires 1–2 spikes with fixed delay when surprised by bright flashes, but this response habituates very rapidly. No response was obtained with pattern movement of any kind. The dendritic structure of this neuron, es-

pecially its dendritic connections with several different central neuropils, suggests that sensory modalities other than visual may contribute to the characteristic response of DN3, and that the apparently low responsiveness with purely visual stimulation may be due to the lack of adequate stimulation.

Comparison of the stereogram with the previous two-dimensional reconstruction of the same neuron (Hengstenberg and Hengstenberg 1980) shows how much more can be learned about the structure of neurons by use of three-dimensional reconstruction and stereoscopy.

Further Applications

The examples demonstrated in this article (Figs. 3–11) have been taken from current research on visual interneurons in the fly's brain. Obviously the very same procedure can be used for other problems, where three-dimensional data of arbitrary structures is available in the form of serial sections or serial frames.

a) Electron Microscopy. The same procedure should be applicable for EM serial sections, because the ratio between section thickness and resolution (500 Å/25 Å = 20) is about the same as that of the paraffin sections used for this article (10 μm/0.5 μm = 20). We expect in particular that stereograms with transparent surfaces will be useful to display synaptic complexes etc.

b) Brain Architecture. A further application will be to reconstruct from unspecifically stained serial sections of the fly's brain the outlines of major neuropil areas and fibre tracts. By plotting such outlines faintly, the three-dimensional reconstruction can be kept quite "transparent" and even multiply enclosed and irregularly shaped neuropils can be depicted in their natural spatial relationships. We expect stereograms to help conceptualization of brain architecture and introducing newcomers to this field.

c) Skeleton and Musculature. It is notoriously difficult to visualize how insects move their head, wings, legs, etc. because skeleton and joints are complicated three-dimensional structures, and the muscles usually extend in different directions. Here too, "transparent" stereograms could help to visualize what movement ensues from the contraction of one, or a group of muscles. We plan to reconstruct the neck musculature of the blowfly in order to find out which of the many small muscles in this region (Sandemann and Markl 1980) generate which of the different head movements (Hengstenberg and Sandemann 1982).

d) Free Flight Trajectories. Using slightly modified data acquisition and display programs, the trajectories of free flying insects can be reconstructed in

three dimensions from high-speed films (Bülthoff et al. 1980). Stereograms allow the visualization of the flight path, the change of flight velocity and of body posture for different flight manoeuvers (Bülthoff et al. 1980), for landing on a target (Poggio and Reichardt 1981; Wagner 1981), or for a male chasing a female fly (Wehrhahn et al. 1982). It is particularly interesting to compare in three dimensions the flight path of a real fly with the trajectory predicted by a mathematical model (Fig. 12). This way the accuracy of the model's theoretical framework is easily revealed.

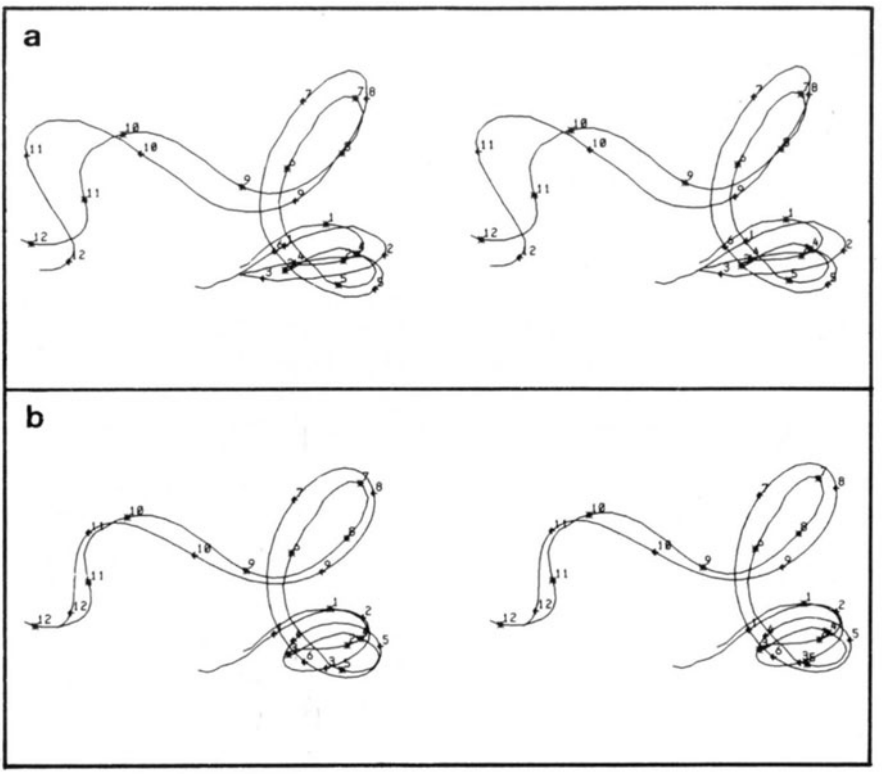

Fig. 12a, b. Free flight trajectories. Stereograms of real and simulated flight paths of two male houseflies, one chasing the other. **a** Flight paths of real flies as reconstructed from a high speed film (80 frames s^{-1}), according to Bülthoff et al. (1980). Corresponding points of the two trajectories are numbered at 100 ms intervals. **b** Flight path of the real, leading fly, and the simulated chasing fly according to an algorithm described by Poggio and Reichardt (1981). The model computes from the 3D-coordinates of the leading fly the future torque, lift and thrust of the chasing male, translates them into angular-, vertical-, and forward velocities, and integrates these into a three-dimensional trajectory. Notice that the "artificial fly", as well as the real one, can accurately follow sharp turns and loopings of the leading fly

Concluding Remarks

Our intention was to develop a simple, computer-assisted method for reconstructing and displaying neural structures in three dimensions using standard equipment. We employed simple procedures transparent enough for people with little experience with computers to use them straight away. We also wanted to find out how much of an "ideal" three-dimensional reconstruction could be achieved by computation of stereograms using only contour data but no sophisticated data processing. Our procedure was developed for analyzing dye-injected visual interneurons of the fly. Its handiness and performance were tested against the usual manual reconstruction procedures, and against results achieved by cobalt mass-fillings of neurons. We have now entirely abandoned manual reconstruction in favour of the computer-assisted procedure.

Control of the acquisition program HISDIG is self-explanatory and foolproof. The reproduction program HISTRA can be handled equally simply. It allows various useful transformations, such as computation of stereograms. These operations are controlled by a plain language dialogue.

With thick sections our use of contour data prohibits image rotation by 90 degrees because the low resolution in the z-direction (given by the section thickness) yields only poor reconstructions. With thinner sections ($1-3\ \mu$m) this drawback becomes less prominent, and rotation up to 60 degrees may be possible (E. Buchner, unpubl.). However, in many cases stereograms eliminate the need for orthogonal projections. At high resolution, they show clearly and in fine detail the three-dimensional structure of neurons and their spatial relationships with other structures. Somewhat to our surprise there seems to be no need to reconnect cut fibres explicitly or to remove hidden contours by special subprograms. Apparently the superb image processor in the observer's brain performs these operations rapidly and reliably.

We now consider our procedure sufficiently developed to be distributed. Operation can be learned within one day. The same system can be realized de novo at an estimated cost of less than US $ 15,000. If a minicomputer or even a microprocessor with suitable peripherals is available, only the digitizer tablet needs to be added. Readers wanting to set up a 3D-reconstruction system may contact us for advice and more detailed information.

Finally, we believe that the heuristic value of stereoscopy for neuroanatomical studies has been deplorably underestimated. The possibility of displaying, together, many complex shapes, combined with our own outstanding abilities of form and depth perception, enormously help the analysis of neural structures.

Acknowledgements. We wish to thank Prof. K. G. Götz, Drs. R. Cook, E. Buchner, K. Hausen, Mr. J. Pagel and U. Wandel for critical advice and help during this work. May 1982